Quasi-one-dimensional harmonically trapped quantum droplets

Dmitry A. Zezyulin School of Physics and Engineering, ITMO University, St. Petersburg 197101, Russia (Dated: March 31, 2023)

We theoretically consider effectively one-dimensional quantum droplets in a symmetric Bose-Bose mixture confined in a parabolic trap. We systematically investigate ground and excited families of localized trapped modes which bifurcate from eigenstates of the quantum harmonic oscillator as the number of particles departs from zero. Families of nonlinear modes have nonmonotonous behavior of chemical potential on the number of particles and feature bistability regions. Excited states are unstable close to the linear limit, but become stable when the number of particles is large enough. In the limit of large density, we derive a modified Thomas-Fermi distribution. Smoothly decreasing the trapping strength down to zero, one can dynamically transform the ground state solution to the solitonlike quantum droplet, while excited trapped states break in several moving quantum droplets.

PACS numbers:

I. INTRODUCTION

Formation of liquidlike quantum droplets in weakly interacting Bose-Bose mixtures is a remarkable manifestation of the beyond-meanfield effects [1]. In threedimensional mixtures, the existence of quantum droplets becomes possible due to the presence of quantum fluctuations which stabilize the system against collapse. At the same time, the liquid phase also persists in lowdimensional geometries [2]. Quantum droplets have been created in several experiments with two-component mixtures [3–7] (and, prior to that, atomic droplets stabilized by quantum fluctuations have been realized in singlecomponent gases of dipolar atoms [8–11]). The beyondmeanfield corrections that enable formation of quantum droplets in a two-component mixture can be taken into account using a system of two Gross-Pitaevskii (GP) equations (or using a single equation, in the case of symmetric mixture), whose specific form heavily depends on the effective dimensionality of liquid [1, 2] and is essentially different from the previously studied GP equations with cubic or cubic-quintic nonlinearity [12, 13]. Effectively one-dimensional (1D) quantum droplets have been studied in several works [14–22]. In particular, it has been found that these states feature solitonlike behavior and rich dynamics [14]. A recent study [22] presents the analysis of kinks and holes nestling in the spatially extended binary mixture. Solutions of this type can be interpreted as counterparts of conventional dark solitons [23, 24]. Multidimensional quantum droplets have also been in the focus of active recent research, see e.g. [25– 30] and review papers [31–33].

A particularly interesting topic is an effect of external trapping on the properties of quantum droplets. For multidimensional quantum droplets in dipolar gases confined in a harmonic trap, it has been found that the resulting ground state phase diagram can feature a region of multistability [34]. Modulational instability in trapped dipolar Bose-Einstein condensates (BECs) leads to formation of multiple droplets [35]. For quantum droplets in binary mixtures, annular potentials can facilitate the formation

of rotating multidimensional droplets [26, 27]. Formation and dynamics of quantum droplets of bosonic mixtures loaded in 1D optical lattices has been studied in [36] and [17]. Various aspects related to the effectively nonlinear behavior of quantum droplets, such as the onset of instabilities, bifurcations of nonlinear states from the linear limit, adiabatic excitation of quantum droplets, and symmetry-breaking have been explored for potentials of different shapes [37, 38].

In the meanfield theory of BECs, it is well known that, apart from the fundamental ground state, externally trapped condensates can also exist in the so-called nonground (or excited) states [39–41]. The first (singlenode) nonground state can be interpreted as a trapped dark soliton [24] in the effectively 1D geometry or as a vortex state [42] in the 2D geometry. Experimental realization of these states can be achieved using the phaseimprinting method [23, 43]. More complex excited states have wavefunctions with incrementally increasing number of zeros and can be considered as nonlinear states of the macroscopic quantum oscillator [44]. Various properties of such trapped excited states have been systematically considered in numerous publications for 1D (cigarshaped) geometry [44–53] as well as for multidimensional cases, see in particular [54-65] and collections of available results in [25, 42, 66, 67]. The excited states can be dynamically stable [52, 53, 65] and perform persistent periodic motion around center of the trap [68–70].

Vast body of knowledge accumulated for trapped BECs naturally suggests to deepen our understanding of the role of external confinement in the formation and behavior of quantum droplets and, in particular, to explore in a more systematic way the corresponding nonground states that can potentially emerge in the presence of the confinement. In this paper, we aim to perform a systematic study of one-dimensional quantum droplets in a symmetric Bose-Bose mixture loaded in a harmonic (parabolic) potential. Apart from the ground nodeless states, the resulting system admits a sequence of families of excited states whose wavefunctions have the incrementing number of zeros and bifurcate from the eigen-

states of the quantum harmonic oscillator. We demonstrate that in the presence of the trapping either the ground state family and the excited families have bistability regions, where stable states with different numbers of particles coexist at the same value of the chemical potential. Peculiar spectrum of the quantum harmonic oscillator results in the instabilities of small-amplitude quantum droplets from the excited families. These instabilities, however, disappear as the number of particles increases above a certain threshold. In the large-density limit, the trapped states can be described by a modified Thomas-Fermi approximation. Numerical simulations of dynamics indicate that smooth decrease of the trapping strength down to zero transforms the ground state to the solitonlike quantum droplet, and nonground states break into several quantum droplets moving with different velocities. We also simulate periodic motion of the quantum droplets around the center of the trap. Several similarities and dissimilarities are found between the trapped beyond-meanfield system and the model with conventional cubic interactions, as well as in comparison to the effectively 1D model with the beyond-meanfield corrections but without the trap.

Organization of the paper is as follows. In the next Section II we formulate the governing model equation. Section III presents a detailed study of stationary modes, and Section IV addresses several dynamical scenarios corresponding to the found states. Concluding Section V summarizes the main results and briefly outlines possible directions for future work.

II. MODEL

In the effectively 1D geometry, formation of liquid droplets results from the balance between the meanfield repulsive contribution to the energy per particle and a beyond-meanfield attractive correction. In case of the symmetric mixture of two species (\uparrow and \downarrow), the dynamics can be described by a single modified GP equation. Assuming that atoms are harmonically confined in a quasi-1D (i.e., cigar-shaped) geometry with the transverse trapping frequency ω_{\perp} being much larger that the frequency of the longitudinal trapping ω_0 , we use the following model [2, 14]

$$i\hbar\Psi_{t} = -\frac{\hbar^{2}}{2m}\Psi_{xx} - \frac{\sqrt{2m}}{\pi\hbar}g^{3/2}|\Psi|\Psi + \delta g|\Psi|^{2}\Psi + \frac{m}{2}\omega_{0}^{2}x^{2}\Psi, \quad (1)$$

where $g=g_{\uparrow\uparrow}=g_{\downarrow\downarrow}>0$ is the repulsive intraspecies coupling coefficient, and $\delta g=g_{\uparrow\downarrow}+\sqrt{g_{\uparrow\uparrow}g_{\downarrow\downarrow}}$ gives the difference between the intracpecies repulsion and intraspecies attraction $g_{\uparrow\downarrow}<0$. We assume $\delta g>0$. In order to present our main results, we transform Eq. (1) into the dimensionless form adopting characteristic units and normalization of the wavefunction that result in equal coef-

ficients in front of the nonlinear terms [14]:

$$x = \frac{\pi \hbar^2 \sqrt{\delta g}}{2mg^{3/2}} x', \quad t_0 = \frac{\pi^2 \hbar^3 \delta g}{2mg^3} t',$$
 (2)

where x' and t' are dimensionless variables, and

$$\Psi = \frac{\sqrt{2m}g^{3/2}}{\pi\hbar\delta g}\Psi'. \tag{3}$$

Rewriting Eq. (1) and omitting primes we arrive at the following normalized equation

$$i\Psi_t = -\Psi_{xx} + \nu^2 x^2 \Psi - |\Psi|\Psi + |\Psi|^2 \Psi,$$
 (4)

where $\nu = \hbar^3 \pi^2 \delta g \omega_0 / (4 m g^3)$ is a dimensionless coefficient that governs the parabolic trap strength.

In what follows, we analyze a slightly more general model that explicitly contains nonlinear coefficients $\sigma_2 \geq 0$ and $\sigma_3 \geq 0$ in front of the nonlinear terms:

$$i\Psi_t = -\Psi_{xx} + \nu^2 x^2 \Psi - \sigma_2 |\Psi| \Psi + \sigma_3 |\Psi|^2 \Psi.$$
 (5)

While we bear in mind that the default case corresponds to $\sigma_2 = \sigma_3 = 1$, the relevance of Eq. (5) is justified by the fact that the generalization to other values of σ_2 and σ_3 is technically simple and yet may yield some additional understandings.

Temporal dynamics governed by Eq. (5) conserves quantities $N = \int_{-\infty}^{\infty} |\Psi|^2 dx$ and

$$E = \int_{-\infty}^{\infty} \left(|\Psi_x|^2 + \nu^2 x^2 |\Psi|^2 - \frac{2\sigma_2}{3} |\Psi|^3 + \frac{\sigma_3}{2} |\Psi|^4 \right) dx, (6)$$

which give the number of atoms and total energy for each component of the mixture, respectively (with the normalization explained below).

III. STATIONARY MODES

A. Families of nonlinear modes

Stationary nonlinear modes for Eq. (5) admit the representation $\Psi(x,t)=e^{-i\mu t}\psi(x)$, where μ is the dimensionless chemical potential. Spatial shape of the stationary wavefunction $\psi(x)$ is determined by the following equation:

$$\psi_{xx} + (\mu - \nu^2 x^2)\psi + \sigma_2 |\psi|\psi - \sigma_3 \psi^3 = 0, \tag{7}$$

subject to the zero boundary conditions at infinity: $\lim_{x\to\pm\infty}\psi(x)=0$. The case $\nu=0$ and $\sigma_2=\sigma_3=1$ was in detail analyzed in [2, 14]. In this case an explicit solitonlike solution is available which has the form $\psi_s(x)=-3\mu[1+\sqrt{1+9\mu/2}\cosh\sqrt{-\mu x^2}]^{-1}$. It exists within the finite interval of chemical potentials $\mu\in(-2/9,0)$, such that $\lim_{N\to0^+}\mu(N)=0$ and $\lim_{N\to\infty}\mu(N)=-2/9$.

In the linear case $\sigma_2 = \sigma_3 = 0$, Eq. (7) transforms to an eigenvalue problem whose spectrum is well-known.

It consists of a sequence of equidistantly spaced discrete eigenvalues which can be listed in the ascending order as $\tilde{\mu}_n = \nu(2n+1)$, where index $n=0,1,\ldots$ enumerates the eigenstates. The corresponding eigenfunctions $\tilde{\psi}_n(x)$ read

$$\tilde{\psi}_n(x) = \sqrt[4]{\nu} H_n(\sqrt{\nu}x) e^{-\nu x^2/2} / \sqrt{\sqrt{\pi} 2^n n!},$$
 (8)

where $H_n(x)$ are Hermite polynomials [71]. Equation (8) implies the normalization $\int_{-\infty}^{\infty} \tilde{\psi}_n^2 dx = 1$. (Notice that hereafter we use tildes to distinguish the solutions that pertain to the linear case).

Regarding the nonlinear stationary equation (7), for the case of meanfield nonlinearity ($\sigma_2 = 0$) it is rather well-known [44, 46, 49, 52] that families of nonlinear modes branch off from the trivial zero solution $\psi(x) \equiv 0$ at $\mu = \tilde{\mu}_n$. To designate the corresponding bifurcation, we will sometimes say that nonlinear modes bifurcate from the linear limit. Looking for a similar bifurcation for trapped quantum droplets described by Eq. (7) with $\sigma_2 \neq 0$, we use the following perturbation expansions for small-amplitude nonlinear modes:

$$\psi_n(x) = \varepsilon \tilde{\psi}_n + \varepsilon^2 \psi_n^{(2)} + \varepsilon^3 \psi_n^{(3)} + \dots, \tag{9}$$

$$\mu_n = \tilde{\mu}_n + \varepsilon \mu_n^{(1)} + \varepsilon^2 \mu_n^{(2)} + \dots,$$
 (10)

where $\varepsilon \ll 1$ is a small real parameter whose meaning is evident: close to the bifurcation, for the number of particles corresponding to ψ_n we have $N_n = \int_{-\infty}^{\infty} \psi_n^2 dx = \varepsilon^2 + o(\varepsilon^2)$. Proceeding in the standard way, we substitute expansions (9)–(10) to Eq. (7) and collect the terms having equal powers of ε . While at the order ε the resulting equation is satisfied automatically, at the order ε^2 we obtain $(\partial_x^2 + \tilde{\mu}_n - \nu^2 x^2)\psi_n^{(2)} = -\mu_n^{(1)}\tilde{\psi}_n - \sigma_2|\tilde{\psi}_n|\tilde{\psi}_n$. The solvability condition for the latter equation requires its right-hand side to be orthogonal to $\tilde{\psi}_n$. This requirement determines the leading correction to the chemical potential:

$$\mu_n^{(1)} = -\sigma_2 \int_{-\infty}^{\infty} \tilde{\psi}_n^2 |\tilde{\psi}_n| dx. \tag{11}$$

The latter coefficient is obviously nonzero, and, close to the bifurcation point, the dependence of the nonlinearity-induced shift of chemical potential on the number of particles N_n is nearly square-root: $\mu - \tilde{\mu}_n \approx \mu_n^{(1)} \sqrt{N_n}$, which is in contrast to the linear law $|\mu - \tilde{\mu}_n| \propto N_n$ in the case of cubic interactions and the power law $|\mu| \propto N^{2/3}$ for 1D quantum droplets without the trapping potential [14]. For $\sigma_2 > 0$ the coefficient $\mu_n^{(1)}$ is obviously negative, which means that sufficiently close to the bifurcation, i.e., for $0 < N_n \ll 1$, chemical potential of the nonlinear family μ_n is less than that of the linear mode: $\mu_n < \tilde{\mu}_n$. This behavior is typical for BECs dominated by the attractive nonlinearity. However, it can be expected that as the effective nonlinearity becomes stronger, the system will be dominated by the cubic repulsive nonlinearity for which the typical behavior is $d\mu/dN > 0$.

The nonmonotonous behavior of the chemical potential μ on number of particles N has indeed been observed for numerically obtained stationary modes, either for the family of ground states and for families of excited states. In left panels of Fig. 1 we plot families of stationary modes bifurcating from four linear eigenstates (n = 0, 1, 2, 3) and visualized as dependencies $\mu_n(N_n) - \tilde{\mu}_n$. In our numerical simulations we have considered harmonic trapping of two different strengths: $\nu^2 = 1$ ("strong trap") and $\nu^2 = 0.01$ ("weak trap"). For comparison, in Fig. 1 we additionally plot the analogous dependence for quantum droplets with zero trapping $\nu^2 = 0$, where $\mu(N)$ is a monotonously decreasing function. As expected from the above considerations, in the presence of the trapping each dependence $\mu_n(N_n)$ is nonmonotonous and has a number of particles N_n^* , where the chemical potential acquires its mimimal value $\mu_n(N_n^*) = \mu_n^*$. For each family the difference between the chemical potential of the corresponding linear state $\tilde{\mu}_n$ and the minimal chemical potential μ_n^* has approximately the same value: $\Delta_n := \tilde{\mu} - \mu_n^* \approx 0.24$. Moreover, this "universal" value does not change much subject to the change of the trap strength (compare the curves for strong and weak trapping). The numerical estimate $\Delta_n \approx 0.24$ is rather close to the analytical value $2/9 \approx 0.22$ that limits the existence range of chemical potentials in the absence of the confinement. In the meantime, the number of particles N_n^* , where the minimal chemical potential μ_n^* is achieved, is appreciable different for the considered trap strengths: for weak trap the minimum of μ_n^* is achieved at larger number of particles. For fixed trap strength, the sequence of critical numbers of particles N_n^* is increasing: in particular, for the strong trap we get $N_0^* \approx 0.57, N_1^* \approx 0.77, N_2^* \approx 0.91,$ $N_3^* \approx 0.99$. The existence of a global minimum of chemical potential can have implications for thermodynamic properties of the condensate. Indeed, since for families of stationary states we have $\mu_n = \partial E_n/\partial N_n$, where E_n is the energy defined by (6), then around the point N_n^* the dependence E(N) has zero curvature: $E(N_n) =$ $E(N_n^*) + \mu_n^*(N_n - N_n^*) + O((N_n - N_n^*)^3)$. Since for each family the dependence $E_n(N_n)$ is a monotonously increasing function [plotted in Fig. 2(a)], the existence of extrema N_n^* allows to find pairs of nonlinear states with equal chemical potentials but different energies.

In right panels of Fig. 1 we show the mean-square width of nonlinear modes defined as $W_n = \sqrt{N_n^{-1} \int_{-\infty}^{\infty} x^2 |\psi_n|^2 dx}$. The dependencies $W_n(\mu_n)$ are also nonmonotonous, but the numbers of particles corresponding to the droplets of minimal size are different from those corresponding the minimal chemical potentials (at the same time, for different families and fixed trap strength the minimal width is achieved for approximately the same number of particles). The nonmonotonous dependence of the meansquare width on the number of particles is similar to that for untrapped solitonlike quantum droplets (see the downmost panel in the right column of Fig. 1). However, in contrast to the case

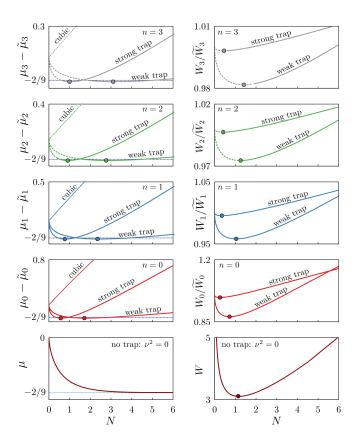


FIG. 1: Dependencies of chemical potential μ (on the left) and meansquare width W (on the right) on the number of particles N for the solitonlike quantum droplet with no trapping (lower panels, $\nu^2 = 0$) and for several families (n = 0, 1, 2, 3) in the presence of harmonic trap of two difference strengths: "strong trap" $\nu^2 = 1$ and "weak trap" $\nu^2 = 0.01$. For trapped states, each panel shows the difference $\mu_n - \tilde{\mu}_n$, where $\tilde{\mu}_n$ is the nth eigenvalue of the linear problem. For widths of trapped states, we plot ratios W_n/\widetilde{W}_n , where \widetilde{W}_n is the width of the corresponding linear eigenfunction $\tilde{\psi}_n$. Small circles show minima of the curves. For comparison, in panels with chemical potentials we plot the analogous dependencies for purely cubic meanfield nonlineaity. For curves labeled as "cubic" we have $\sigma_2 = 0$, $\sigma_3 = 1$ and for all other curves $\sigma_2 = \sigma_3 = 1$. Solid and dotted fragments of plotted curves correspond to stable and unstable solutions, respectively. This figure shows only the behavior near the linear limit, i.e., for relatively small number of particles N. A "global" picture for larger numbers of particles is presented in Fig. 3.

of zero trap, in the linear limit $N \to 0$ the widths of trapped states remain finite and do not diverge.

While Fig. 1 zooms in the behavior of nonlinear modes close to the linear limit, in Fig. 3(a) we present a more global diagram which shows the behavior of nonlinear modes in the region of strong effective nonlinearity. In the limit $\mu \gg 1$ and $N \gg 1$ (i.e., the Thomas-Fermi (TF) limit [12, 13]), the large-density modes are dominated by the cubic nonlinearity. Using $\mu^{-1/2}$ as a small parameter, we observe that in the leading order the TF

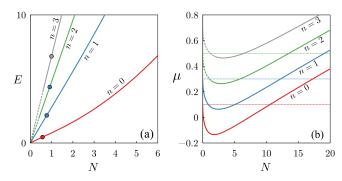


FIG. 2: (a) Dependencies of energy E on number of particles N for several lower families of nonlinear modes (n=0,1,2,3) in the presence of strong harmonic trap $\nu^2=1$. Circles correspond to the points $N=N_n^*$ of zero curvature, where $\partial^2 E(N_n^*)/\partial N^2=0$. (b) Dependencies $\mu(N)$ in the weak trap $\nu^2=0.01$. Thin horizontal lines correspond to chemical potentials of linear states. In both panels, solid and dotted fragments of plotted curves correspond to stable and unstable solutions, respectively. In this figure $\sigma_2=\sigma_3=1$.

distribution of the ground state family coincides with the standard one [12], i.e., $\psi_{0,TF}^2 = \sigma_3^{-1}(\mu - \nu^2 x^2)$ for x lying within the TF radius: $|x| \leq \nu^{-1} \sqrt{\mu}$. Taking into account the next order of the asymptotic series, we find that the beyond-meanfield correction leads to the following modification of the TF ground state solution:

$$\psi_{0.TF}^2 \approx \sigma_3^{-1} (\mu - \nu^2 x^2 + \sigma_2 \sqrt{\mu - \nu^2 x^2} / \sqrt{\sigma_3}),$$
 (12)

which is illustrated in Fig. 3(b). The number of particles corresponding to the modified TF distribution (12) amounts to

$$N_{0,TF} = (\sigma_3 \nu)^{-1} \left(\frac{4}{3} \mu^{3/2} + \frac{\pi \sigma_2}{2\sqrt{\sigma_3}} \mu \right).$$
 (13)

Therefore, although the beyond-meanfield correction does not change the TF radius, it results in the positive (and linear in μ) addition to the number of particles (which might seem counterintuitive in view of the fact that the nonlinear terms proportional to σ_2 and σ_3 are competing).

B. Bistability of trapped states

Let us now proceed to discussion of stability of stationary nonlinear modes. Standard procedure of linear stability analysis (see Appendix A) indicates that dynamical behavior of small-amplitude perturbations on top of the nonlinear mode is determined by the spectrum of the following eigenvalue problem:

$$\Lambda \zeta = L^+ L^- \zeta,\tag{14}$$

where

$$L^{\pm} = \partial_x^2 + \mu - \nu^2 x^2 + \frac{\sigma_2}{2} (3 \pm 1) |\psi| - \sigma_3 (2 \pm 1) \psi^2, (15)$$

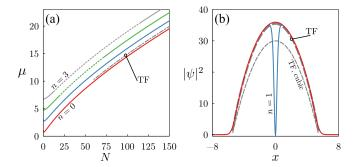


FIG. 3: (a) Dependencies of chemical potential μ on number of particles N for several families of nonlinear modes (n=0,1,2,3) in the presence of the harmonic trap. Solid and dotted fragments correspond to stable and unstable solutions, respectively. Dash-dotted line labelled as 'TF' shows the dependence (13) obtained analytically for the ground state family in the Thomas-Fermi limit. (b) Nonlinear modes for n=0 and n=1 at $\mu=30$. Bold dashed line labelled as 'TF' shows the analytical profile in the Thomas-Fermi limit obtained from Eq. (12). For comparison, with thin dashed line labelled as "TF cubic" we show the conventional Thomas-Fermi cloud [12] $\mu-\nu^2x^2$. In this figure, we consider strong trap $\nu^2=1$ and $\sigma_2=\sigma_3=1$.

 Λ is the eigenvalue, and $\zeta=\zeta(x)$ is the corresponding eigenfunction. Stationary mode $\psi(x)$ is said to be stable if all eigenvalues Λ are real and nonnegative. Otherwise the solution $\psi(x)$ is said to be unstable, and the growth rate of the exponential dynamical instability is determined by the positive imaginary part $\mathrm{Im}\sqrt{\Lambda}$. Eigenvalue problem (14) has two evident analytic solutions. The first one corresponds to $\Lambda=0$ with eigenfunction $\zeta=\psi(x)$ and obviously reflects the invariance of the model under the phase rotation. The second analytical solution (which is the peculiarity of the parabolic potential) is given as $\Lambda=4\nu^2$ and $\zeta=x\psi(x)$ [52, 70] and proves to be useful for understanding of linear stability of small-amplitude nonlinear modes.

The equidistant spectrum of the parabolic potential results in the specific stability picture of small-amplitude nonlinear states [52]: for small-amplitude modes bifurcating from the nth linear state, the stability spectrum in the linear limit contains exactly n double eigenvalues that result from the "resonances" between different intrinsic modes. When small-amplitude nonlinear states branch off from the linear limit, each double eigenvalue splits either into a pair of real eigenvalues or into a complex-conjugate pair, and the latter situation implies that the bifurcating small-amplitude modes are unstable. Splittings of double eigenvalues can be analyzed using the perturbation theory which was previously used in several similar situations [52, 65, 72–74] and, for self-containment of our paper, is summarized in Appendix A. The results of the perturbation analysis for small-amplitude modes can be outlined as follows. For the lowest family, n=0, there is no double eigenvalues

in the spectrum, and therefore small-amplitude ground states are stable. For the single-node family, n = 1, there is exactly one double eigenvalue equal to $\Lambda = 4\nu^2$. Splitting of this double eigenvalue into a complex-conjugate pair is a priori impossible due to the presence of the exact solution mentioned above (because the eigenvalue $\Lambda = 4\nu^2$ must always be present in the spectrum), and therefore the single-node states are also stable close to the linear limit. For n=2 there are two double eigenvalues situated at $\Lambda = 4\nu^2$ and $\Lambda = 16\nu^2$, and the latter one does split into a complex-conjugate pair, which means that the small-amplitude solutions of this family are unstable. Similar instability also takes place for families n=3 and n=4 (we hypothesize that all families with larger n are also unstable near the linear limit). From the perturbation theory it is evident that when the dynamical instability is present, its increment is proportional to ε and, respectively, proportional to $N^{1/2}$. This behavior is different from the purely cubic case, where the instability increment of small-amplitude modes is proportional to N [52, 74].

We further employ the numerical solution of the eigenvalue problem (14) to address the stability of nonlinear modes of larger amplitude, see Figs. 1, Fig. 2(a), and 3(a), where solid and dotted fragments of plotted curves correspond to stable and unstable nonlinear modes, respectively. Regarding, the ground state family n = 0and the single-node family n=1, we observe that their solutions remain stable for modes of any arbitrary amplitude. This, in particular, means that these families feature bistability regions, where the same family of nonlinear modes has two stable states with equal chemical potentials but different numbers of particles. Similar bistability has been earlier encountered for a BEC with spatially inhomogeneous scattering length [75] and for self-sustained [76] and guided [77] solitons in the cubicquintic medium. We emphasize that in the case at hand the bistability takes place exactly due to the presence of the confining potential, since for zero trapping strength the dependence $\mu(N)$ is monotonous [14], see also the plot $\mu(N)$ for $\nu^2 = 0$ in Fig. 1.

Proceeding to the numerical study of next families n=2 and n=3, we confirm that close to the linear limit nonlinear states are unstable, see the corresponding panels in Fig. 1. In the meanwhile, the increase of the number of particles N leads to the stabilization of these families. In terms of the linear stability spectrum, such a stabilization corresponds to a moment when the complex-conjugate pair of unstable eigenvalues returns to the real axis. The change from instability to stability occurs for the number of particles less than that corresponding to the minimal value of the chemical potential. This means that these families also contain intervals of bistable chemical potentials, although these intervals are more narrow than those for the two lowest families with n=0 and n=1. For larger numbers of particles, families n=2 and n=3 have additional finite instability windows which are not shown in Fig. 1, but become visible in the more global diagram presented in Fig. 3(a). However, for sufficiently large N these families again become stable, which could be expected from the stability analysis in the TF limit (with purely cubic nonlinearity) performed in [53]. We also notice that in the case at hand the change of the slope $d\mu/dN$ from negative to positive does not result in the stability change [78] (as it often happens in other nonlinear wave systems, where the Vakhitov-Kolokolov stability condition [79] ensures that the solution is unstable when $d\mu/dN > 0$).

The fact that the difference Δ_n between the linear eigenvalue $\tilde{\mu}_n$ and the minimal chemical potential μ_n^* weakly depends on the strength of the trapping implies that the two considered trap strengths correspond to different situations. Indeed, the chemical potentials of linear eigenstates form an equidistant sequence: $\Delta\mu:=\tilde{\mu}_{n+1}-\tilde{\mu}_n=2\nu$, and for the strong trap $\nu^2\gtrsim 1$ the difference between the linear eigenvalues is much larger than the difference $\Delta_n\approx 0.24$, i.e., $2\nu\gg\Delta_n$. However, for the weak trap $\nu^2\ll 1$, the inequality $2\nu<\Delta_n$ takes place. In this case the linear eigenvalue $\tilde{\mu}_n$ (which can be considered as a chemical potential for a gas of noniteracting particles in the harmonic trap) belongs to the interval of bistable chemical potentials of the next family with n+1. This situation is illustrated in Fig. 2(b).

IV. SIMULATIONS OF DYNAMICS

Nonlinear dynamics of found stationary states has been simulated by integrating the time-dependent GP equation (5) with a split-step method. To examine the dynamical (bi)stability of stationary states, we solve the initial value problem with the initial condition taken in the form of the stationary wavefunction perturbed by a random noise: $\Psi(t=0,x) = \psi(x)[1+0.025(r_1(x)+ir_2(x))],$ where perturbations $r_{1,2}$ are obtained as normally distributed pseudorandom numbers. These simulations confirm the existence of bistable states on the lowest (n = 0)and the first excited (n = 1) families. Regarding the next families, n=2 and n=3, in accordance with the linear stability predictions, we have observed that smallamplitude nonlinear modes are unstable. However, as the amplitude (i.e., number of particles) becomes large enough, the solutions become stable. This difference in stability of excited states of different amplitudes is illustrated in Fig. 4, where unstable and stable dynamics are visualized for nonlinear states coexisting at equal values of the chemical potential.

Apart from the direct stability tests, we have addressed several other dynamical scenarios. In particular, we ran a series of simulations where the strength of the trapping potential $\nu^2 = \nu^2(t)$ was smoothly decreased down to zero. In this case the nonlinear mode that initially belonged to the ground state family transformed to a solitonlike quantum droplet, while a nonlinear mode from the first family (n=1) decoupled in a pair of mutually repulsing droplets of identical form. These results are

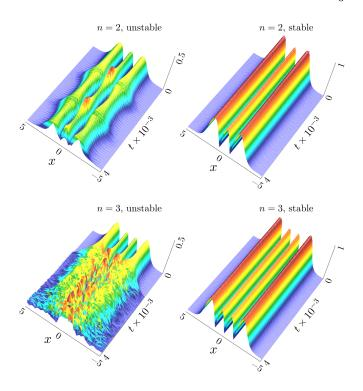


FIG. 4: Plots $|\Psi(x,t)|$ for nonlinear dynamics corresponding to stationary modes with n=2 (upper panels, solutions at $\mu \approx 4.831$) and n=3 (lower panels, solutions at $\mu \approx 6.822$). Solutions of smaller amplitudes are unstable, and those with larger amplitudes are stable. Here $\nu^2=1$, and $\sigma_2=\sigma_3=1$.

illustrated in Fig. 5(a) and (b), respectively. Similar behavior can be observed for further families. For instance, Fig. 5(c) shows how the localized mode from the family n=2 breaks into three droplets, one of which is quiescent while two others are moving in opposite directions. As becomes evident from Fig. 5(d), in this case the amplitude of moving droplets is slightly larger than that of the quiescent central droplet. In a similar way, the initially trapped localized state from the family n=3 fans into four droplets: two moving to the right with different velocities and two others moving to the left [see Figs. 5(e-f)].

It is known that any stationary mode $\psi(x)$ of the GP equation with the harmonic potential generates a family of periodically moving solutions given by the explicit formula [80, 81] $\Psi(x,t) = \psi(x-X(t))e^{-i\mu t+i\dot{X}(t)x/2}$, where X(t) is an arbitrary solution of the differential equation $\ddot{X}+2\nu^2X=0$ (here dot and double dot denote first and second derivatives in time t). Clearly, X(t) can be interpreted as a center-of-mass of the oscillating solution. Exact solutions of this form enable the systematic investigation of periodically moving quantum droplets. Moreover, assuming that the initial condition is prepared as a superposition of two well-separated quantum droplets: $\Psi(x,t=0)=\psi_1(x-X_1(0))e^{i\dot{X}_1(0)x/2}+\psi_2(x-X_2(0))e^{i\dot{X}_2(0)x/2}$, $|X_1(0)-X_2(0)|\gg 1$, it is possible to

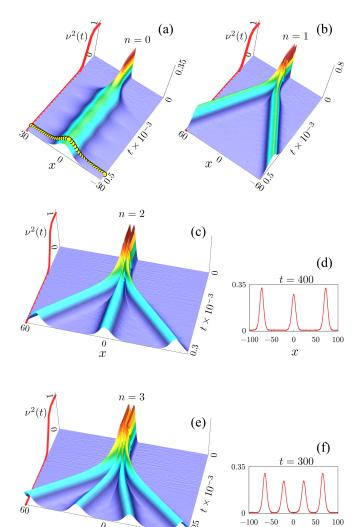


FIG. 5: Plots $|\Psi(x,t)|$ for nonlinear dynamics corresponding to initial condition chosen as a stationary mode with n=0,1,2,3 as the harmonic trap strength $\nu^2(t)$ is smoothly decreased from 1 to 0. Dependencies $\nu^2(t)$ are plotted with bold curves. Dots in (a) show the profile of the solitonlike quantum droplet at $\nu^2=0$ corresponding to the number of particles equal to that of the initial condition; (d) and (e) show shapshots of solutions with n=2 and n=3 taken at t=400 and t=300, respectively.

-60

simulate the dynamics corresponding to simultaneous oscillations of two droplets in the same trap. In Fig. 6 we present two examples of composite oscillating solutions. While preliminary numerical simulations suggest that the periodic movement robustly persists for indefinite time, an accurate stability study for the oscillating droplets is a relevant task for future work. For the GP equation with the meanfield cubic nonlinearity such a surprisingly regular behavior of a pair of colliding harmonically-trapped ground states has been earlier documented in [81] and explained by reducing the GP equation to a dynamical sys-

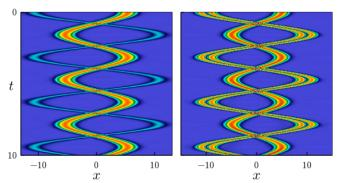


FIG. 6: Pseudocolor plots of composite oscillating solutions composed of two nodeless ground states from the family n=0 having equal chemical potential $\mu=0.82$ and different numbers of particles $N\approx 0.15$ and $N\approx 1.32$ (a), and one ground state with n=0 corresponding to $\mu=0.82$ and $N\approx 1.32$ and one single-node state with n=1 corresponding to $\mu=2.8$ and $N\approx 1.57$ (b). In this figure $\nu=1$, $\sigma_2=\sigma_3=1$.

tem which treats solitary waves as classical particles and happens to be completely integrable in the two-particle case.

V. CONCLUSION

The main goal of our paper has been to develop a systematic analysis of quasi-one-dimensional quantum droplets confined in the parabolic potential. Apart from the fundamental ground states, we have extended the consideration onto the families of nonground excited states which are well-known in the meanfield BEC theory but have received comparatively little attention in the modified model with the beyond-meanfield corrections. The main results of our study can be summarized as follows.

- (1) Apart from the family of trapped ground states, there exists a sequence of excited families. Either the ground state family and excited states bifurcate from eigenstates of the underlying quantum harmonic oscillator and feature nonmonotonous behavior of the chemical potential on the number of particles. Each family has the minimal chemical potential. The difference between the chemical potential in the linear limit and the minimal chemical potential exhibits a remarkable universality, i.e., weakly depends on the family number and on the strength of the parabolic trap.
- (2) Either the ground state family and excited-state families feature a bistability region, where two stable nonlinear modes coexist at the same chemical potential but with different numbers of particles.
- (3) Excited states are unstable close to the linear limit,

but become stable as the number of particles increases.

- (4) In the large-density limit, the trapped states can be described using a modified Thomas-Fermi (TF) distribution which contains larger number of particles than the conventional TF cloud in BECs with purely cubic meanfield repulsion.
- (5) Smooth decrease of the harmonic trap strength dynamically transforms the ground state into a solitonlike quantum droplet, while a single-node trapped state transforms into a pair of parting droplets. More complex trapped states break into multiple droplets.
- (6) Trapped states perform stable oscillations around the center of the trap. A pair of repeatedly colliding trapped states can feature regular dynamics.

These results call for a natural generalization onto the effectively multidimensional geometries, where the formation of trapped vortices and vortex rings and their eventual stabilization using the weak unharmonicity of the trapping potential [58, 65] would be a particularly interesting subject. Another natural extension is to address the role of the confinement in an essentially twocomponent asymmetric mixture, where additional instabilities can emerge [22]. Finally, it can be relevant to explore the effect of the external trapping in the modified theory of quantum droplets which accounts for bosonic pairing [82, 83] and provides a better agreement between the analytical estimate of the quantum droplet energy and diffusion Monte Carlo simulations [2, 18, 19]. The pairing theory is expected to modify the balance between the competing repulsion and attraction in the corresponding effective one-dimensional Gross-Pitaevskii equation and therefore can lead to a quantitative change of the results presented herein.

Appendix A: Linear stability analysis

Using the standard substitution for the perturbed solution $\Psi = e^{-i\mu t}[\psi(x) + \xi(x,t)]$ and performing the linearization of the GP equation (5), we find that the perturbation $\xi(x,t)$ obeys the following equation (we bear in mind that wavefunction ψ is real-valued):

$$i\xi_t = -\xi_{xx} - (\mu - \nu^2 x^2)\xi - \frac{\sigma_2}{2}|\psi|(3\xi + \bar{\xi}) + \sigma_3 \psi^2(2\xi + \bar{\xi}),$$
(A1)

where $\bar{\xi}$ is the complex-conjugate of ξ . Separating the perturbation into real and imaginary parts, $\xi = \chi + i\varphi$,

we obtain a pair of equations $\chi_t = -L^-\varphi$, $\varphi_t = L^+\chi$, where operators L^\pm are given in Eq. (15). Therefore the stability eigenproblem can be written down as $\Lambda\zeta = L^+L^-\zeta$, where Λ is the eigenvalue. The solution is said to be stable if and only if all eigenvalues Λ are real and nonnegative.

Using the pertubation expansions (9)–(10), for stability of nonlinear modes bifurcating from the nth linear eigenstate, we have $L^+L^- = \mathcal{L}_n^2 + \varepsilon M_n + o(\varepsilon)$, where $\mathcal{L}_n = \partial_x^2 + \tilde{\mu}_n - \nu^2 x^2$, and

$$M_n = \mathcal{L}_n(\mu_n^{(1)} + \sigma_2|\tilde{\psi}_n|) + (\mu_n^{(1)} + 2\sigma_2|\tilde{\psi}_n|)\mathcal{L}_n.$$
 (A2)

At $\varepsilon=0$ the linear stability operator becomes equal to \mathcal{L}_n^2 . For each $n=0,1,\ldots$ there are exactly n double (more precisely, semisimple) eigenvalues in the spectrum: $\Lambda_{n,k}=4\nu^2(k-n)^2$, where $k=0,1,\ldots,n-1$ (see [52] for more detailed discussion). As ε departs from zero, each double eigenvalue generically splits into a pair of simple eigenvalues. This process can be described using the expansion $\Lambda_{n,k}^{(1,2)}=4\nu^2(k-n)^2+\varepsilon\omega_n^{(1,2)}+o(\varepsilon)$, where coefficients $\omega_n^{(1,2)}$ are eigenvalues of the 2×2 matrix

$$\tilde{M}_{n,k} = \begin{pmatrix} \langle M_n \tilde{\psi}_k, \tilde{\psi}_k \rangle & \langle M_n \tilde{\psi}_k, \tilde{\psi}_{2n-k} \rangle \\ \langle M_n \tilde{\psi}_{2n-k}, \tilde{\psi}_k \rangle & \langle M_n \tilde{\psi}_{2n-k}, \tilde{\psi}_{2n-k} \rangle \end{pmatrix}.$$

The entries of matrix $\tilde{M}_{n,k}$ can be represented as

$$\begin{split} \langle M_n \tilde{\psi}_k, \tilde{\psi}_k \rangle &= 2\sigma_2(n-k) \int |\tilde{\psi}_n| (3\tilde{\psi}_k^2 - 2\tilde{\psi}_n^2) dx, \\ \langle M_n \tilde{\psi}_k, \tilde{\psi}_{2n-k} \rangle &= -\langle M_n \tilde{\psi}_{2n-k}, \tilde{\psi}_k \rangle \\ &= 2\sigma_2(n-k) \int |\tilde{\psi}_n| \tilde{\psi}_k \tilde{\psi}_{2n-k} dx, \\ \langle M_n \tilde{\psi}_{2n-k}, \tilde{\psi}_{2n-k} \rangle \\ &= -2\sigma_2(n-k) \int |\tilde{\psi}_n| (3\tilde{\psi}_{2n-k}^2 - 2\tilde{\psi}_n^2) dx, \end{split}$$

where $\int = \int_{-\infty}^{\infty}$. Since the eigenfunctions $\tilde{\psi}_n(x)$ are available in the explicit form from Eq. (8), matrices $\tilde{M}_{n,k}$ and their eigenvalues can be found with a computer algebra software.

Acknowledgments

The work was supported by the Priority 2030 Federal Academic Leadership Program.

D. S. Petrov, Quantum Mechanical Stabilization of a Collapsing Bose-Bose Mixture, Phys. Rev. Lett. 115, 155302

^[2] D. S. Petrov and G. E. Astrakharchik, Ultradilute Low-

- Dimensional Liquids, Phys. Rev. Lett. **117**, 100401 (2016).
- [3] C. R. Cabrera, L. Tanzi, J. Sanz, B. Naylor, P. Thomas, P. Cheiney, and L. Tarruell, Quantum liquid droplets in a mixture of Bose-Einstein condensates, Science 359, 301 (2018).
- [4] P. Cheiney, C. R. Cabrera, J. Sanz, B. Naylor, L. Tanzi, and L. Tarruel, Bright Soliton to Quantum Droplet Transition in a Mixture of Bose-Einstein Condensates, Phys. Rev. Lett. 120, 135301 (2018).
- [5] G. Semeghini, G. Ferioli, L. Masi, C. Mazzinghi, L. Wolswijk, F. Minardi, M. Modugno, G. Modugno, M. Inguscio, and M. Fattori, Self-Bound Quantum Droplets of Atomic Mixtures in Free Space, Phys. Rev. Lett. 120, 235301 (2018).
- [6] G. Ferioli, G. Semeghini, L. Masi, G. Giusti, G. Modugno, M. Inguscio, A. Gallemí, A. Recati, and M. Fattori, Collisions of self-bound quantum droplets, Phys. Rev. Lett. 122, 090401 (2019).
- [7] C. D'Errico, A. Burchianti, M. Prevedelli, L. Salasnich, F. Ancilotto, M. Modugno, F. Minardi, and C. Fort, Observation of quantum droplets in a heteronuclear bosonic mixture, Phys. Rev. Research 1, 033155 (2019).
- [8] H. Kadau, M. Schmitt, M. Wenzel, C. Wink, T. Maier, I. Ferrier-Barbut, and T. Pfau, Observing the Rosensweig instability of a quantum ferrofluid, Nature (London) 530, 194 (2016).
- [9] I. Ferrier-Barbut, H. Kadau, M. Schmitt, M. Wenzel, and T. Pfau, Observing the Rosensweig instability of a quantum ferrofluid, Phys. Rev. Lett. 116, 215301 (2016).
- [10] L. Chomaz, S. Baier, D. Petter, M. J. Mark, F. Wächtler, L. Santos, and F. Ferlaino, Quantum-Fluctuation-Driven Crossover from a Dilute Bose-Einstein Condensate to a Macrodroplet in a Dipolar Quantum Fluid, Phys. Rev. X 6, 041039 (2016).
- [11] M. Schmitt, M. Wenzel, F. Böttcher, I. Ferrier-Barbut, and T. Pfau, Self-bound droplets of a dilute magnetic quantum liquid, Nature (London) 539, 259 (2016).
- [12] C. J. Pethick and H. Smith, Bose–Einstein Condensation in Dilute Gases (Cambridge University Press, Cambridge, England, 2001).
- [13] L. P. Pitaevskii and S. Stringari, *Bose-Einstein Condensation* (Clarendon Press: Oxford and New York, 2003).
- [14] G. E. Astrakharchik and B. A. Malomed, Dynamics of one-dimensional quantum droplets, Phys. Rev. A 98, 013631 (2018).
- [15] F. K. Abdullaev, A. Gammal, R. K. Kumar, and L. Tomio, Faraday waves and droplets in quasi-onedimensional Bose gas mixtures, J. Phys. B: At. Mol. Opt. Phys. 52, 195301 (2019).
- [16] S. R. Otajonov, E. N. Tsoy, and F. K. Abdullaev, Stationary and dynamical properties of one-dimensional quantum droplets, Phys. Lett. A 383, 125980 (2019).
- [17] Z. Zhou, X. Yu, Y. Zou, and H. Zhong, Dynamics of quantum droplets in a one-dimensional optical lattice, Commun. Nonlinear Sci. Numer. Simulat. 78, 104881 (2019).
- [18] L. Parisi, G. E. Astrakharchik, and S. Giorgini, Liquid State of One-Dimensional Bose Mixtures: A Quantum Monte Carlo Study, Phys. Rev. Lett. 122, 105302 (2019).
- [19] L. Parisi and S. Giorgini, Quantum droplets in onedimensional Bose mixtures: A quantum Monte Carlo study, Phys. Rev. A 102, 023318 (2020).
- [20] M. Tylutki, G. Astrakharchik, B. A. Malomed, and D. S.

- Petrov, Collective excitations of a one-dimensional quantum droplet, Phys. Rev. A 101, 051601(R) (2020).
- [21] T. Mithun, A. Maluckov, K. Kasamatsu, B. A. Malomed, and A. Khare, Inter-component asymmetry and formation of quantum droplets in quasi-one-dimensional binary Bose gases, Symmetry 12, 174 (2020).
- [22] Y. V. Kartashov, V. M. Lashkin, M. Modugno, and L. Torner, Spinor-induced instability of kinks, holes and quantum droplets, New J. Phys. 24, 073012 (2022).
- [23] S. Burger, K. Bongs, S. Dettmer, W. Ertmer, and K. Sengstock, A. Sanpera, G. V. Shlyapnikov, and M. Lewenstein, Dark Solitons in Bose-Einstein Condensates, Phys. Rev. Lett. 83, 5198 (1999).
- [24] P. G. Kevrekidis, D. J. Frantzeskakis and and R. Carretero-González, The Defocusing Nonlinear Schrödinger Equation: From Dark Solitons to Vortices and Vortex Rings (Philadelphia, PA: SIAM, 2016).
- [25] Y. V. Kartashov, B. A. Malomed, and L. Torner, Metastability of Quantum Droplet Clusters, Phys. Rev. Lett. 122, 193902 (2019).
- [26] M. N. Tengstrand, P. Sturmer, E. Ö. Karabulut, and S. M. Reimann, Rotating binary Bose-Einstein condensates and vortex clusters in quantum droplets, Phys. Rev. Lett. 123, 160405. (2019).
- [27] L. Dong, and Y. V. Kartashov, Rotating Multidimensional Quantum Droplets, Phys. Rev. Lett. 126, 244101 (2021).
- [28] A. Cidrim, F. E. A. dos Santos, E. A. L. Henn, and T. Macrí, Vortices in self-bound dipolar droplets Phys. Rev. A 98, 023618 (2018).
- [29] Y. Li, Z. Chen, Z. Luo, C. Huang, H. Tan, W. Pang, and B. A. Malomed, Two-dimensional vortex quantum droplets Phys. Rev. A 98, 063602 (2018).
- [30] G. Ferioli, G. Semeghini, S. Terradas-Briansó, L. Masi, M. Fattori, and M. Modugno, Dynamical formation of quantum droplets in a 39K mixture, Phys. Rev. Research 2, 013269 (2020).
- [31] Y. V. Kartashov, G. E. Astrakharchik, B. A. Malomed, and Lluis Torner, Frontiers in multidimensional selftrapping of nonlinear fields and matter, Nature Rev. Phys. 1, 185 (2019).
- [32] Zhi-Huan Luo, Wei Pang, Bin Liu, Yong-Yao Li, B. A. Malomed, A new form of liquid matter: Quantum droplets, Front. Phys. 16, 32201 (2021).
- [33] F. Böttcher, J.-N. Schmidt, J. Hertkorn, K. S. N. Ng, S. D. Graham, M. Guo, T. Langen, and T. Pfau, New states of matter with fine-tuned interactions: quantum droplets and dipolar supersolids Rep. Prog. Phys. 84, 012403 (2021).
- [34] F. Wächtler and L. Santos, Ground-state properties and elementary excitations of quantum droplets in dipolar Bose-Einstein condensates, Phys. Rev. A 94, 043618 (2016).
- [35] I. Ferrier-Barbut, M. Wenzel, M. Schmitt, F. Böttcher, and T. Pfau, Onset of a modulational instability in trapped dipolar Bose-Einstein condensates, Phys. Rev. A 97, 011604(R) (2018).
- [36] I. Morera, G. E. Astrakharchik, A. Polls, and Bruno Julía-Díaz, Quantum droplets of bosonic mixtures in a one-dimensional optical lattice, Phys. Rev. Research 2, 022008(R) (2020).
- [37] B. Liu, H. F. Zhang, R. X. Z, X. L. Zhang, X. Z. Qin, C. Q. Huang, Y. Y. Li, and B. A. Malomed, Symmetry

- breaking of quantum droplets in a dual-core trap, Phys. Rev. A 99, 053602 (2019).
- [38] J. Song and Z. Yan, Dynamics of 1D and 3D quantum droplets in parity-time-symmetric harmonic-Gaussian potentials with two competing nonlinearities, Physica D 442, 133527 (2022).
- [39] V. I. Yukalov, E. P. Yukalova, and V. S. Bagnato, Nonlinear coherent modes of trapped Bose-Einstein condensates, Phys. Rev. A 66, 043602 (2002).
- [40] V. I. Yukalov and E. P. Yukalova, Topological coherent modes for nonlinear Schrödinger equation, J. Phys. A: Math. Gen. 35, 8603 (2002).
- [41] V.V. Konotop and P. G. Kevrekidis, Bohr-Sommerfeld Quantization Condition for the Gross-Pitaevskii Equation, Phys. Rev. Lett. 91, 230402 (2003).
- [42] A. L. Fetter and A. A. Svidzinsky, Vortices in a trapped dilute Bose-Einstein condensate, J. Phys.: Condens. Matter. 13, R135 (2001).
- [43] J. Denschlag and J. E. Simsarian and D. L. Feder and Charles W. Clark and L. A. Collins and J. Cubizolles and L. Deng and E. W. Hagley and K. Helmerson and W. P. Reinhardt and S. L. Rolston and B. I. Schneider and W. D. Phillips, Generating Solitons by Phase Engineering of a Bose-Einstein Condensate, Science 287, 97 (2000).
- [44] Yu. S. Kivshar, T. Alexander, and S. K. Turitsyn, Nonlinear modes of a macroscopic quantum oscillator, Phys. Lett. A 278, 225 (2001).
- [45] V. M. Pérez-García, H. Michinel, H. Herrero, Bose-Einstein solitons in highly asymmetric traps, Phys. Rev. A 57, 3837 (1998).
- [46] M. Kunze, T. Küpper, V. K. Mezentsev, E. G. Shapiro, and S. Turitsyn, Nonlinear solitary waves with Gaussian tails, Physica D 128, 273 (1999).
- [47] L. D. Carr, J. N. Kutz, and W. P. Reinhardt, Stability of stationary states in the cubic nonlinear Schrödinger equation: Applications to the Bose-Einstein condensate Phys. Rev. E 63, 066604 (2001).
- [48] R. D' Agosta, B. A. Malomed, and C. Presilla, Stationary stets of Bose-Einstein condensates in single- and multi-well trapping potentials, Laser Phys. 12, 37 (2002).
- [49] P. G. Kevrekidis, V. V. Konotop, A. Rodrigues, and D. J. Frantzeskakis, Dynamic generation of matter solitons from linear states via time-dependent scattering lengths, J. Phys. B: At. Mol. Opt. Phys. 38, 1173 (2005).
- [50] G. Theocharis, P. G. Kevrekidis, D. J. Frantzeskakis, and P. Schmelcher, Symmetry breaking in symmetric and asymmetric double-well potentials, Phys. Rev. E 74, 056608 (2006).
- [51] M. Brtka, A. Gammal, L. Tomio, Relaxation algorithm to hyperbolic states in Gross-Pitaevskii equation, Phys. Lett. A 359, 339 (2006).
- [52] D. A. Zezyulin, G. L. Alfimov, V. V. Konotop, and V. M. Pérez-García, Stability of excited states of a Bose-Einstein condensate in an anharmonic trap, Phys. Rev. A 78, 013606 (2008).
- [53] M. P. Coles, D. E. Pelinovsky, and P. G. Kevrekidis, Excited states in the large density limit: a variational approach, Nonlinearity 23, 1753 (2010).
- [54] H. Pu, C. K. Law, J. H. Eberly, and N. P. Bigelow, Coherent disintegration and stability of vortices in trapped Bose condensates, Phys. Rev. A 59, 1533 (1999).
- [55] J. J. García-Ripoll, G. Molina-Terriza, V. M. Pérez-García, and L. Torner, Structural Instability of Vortices in Bose-Einstein Condensates, Phys. Rev. Lett. 87,

- 140403 (2001).
- [56] L.-C. Crasovan, V. Vekslerchik, V. M. Pérez-García, J. P. Torres, D. Mihalache, and L. Torner, Stable vortex dipoles in nonrotating Bose-Einstein condensates, Phys. Rev. A 68, 063609 (2003).
- [57] L.-C. Crasovan, V. M. Perez-Garcia, I. Danaila, D. Mihalache, Ll. Torner, Three-dimensional parallel vortex rings in Bose-Einstein condensates, Phys. Rev. A 70, 033605 (2004).
- [58] E. Lundh and H. M. Nilsen, Dynamic stability of a doubly quantized vortex in a three-dimensional condensate, Phys. Rev. A 74, 063620 (2006).
- [59] J. A. M. Huhtamäki, M. Möttönen, and S. M. M. Virtanen, Dynamically stable multiply quantized vortices in dilute Bose-Einstein condensates, Phys. Rev. A 74, 063620 (2006).
- [60] D. Michalache, D. Mazilu, B. A. Malomed, F. Lederer, Vortex stability in nearly-two-dimensional Bose-Einstein condensates with attraction, Phys. Rev. A 73, 043615 (2006).
- [61] L. D. Carr and C. W. Clark, Vortices in Attractive Bose-Einstein Condensates in Two Dimensions, Phys. Rev. Lett. 97, 010403 (2006).
- [62] L. D. Carr and C. W. Clark, Vortices and ring solitons in Bose-Einstein condensates, Phys. Rev. A 74, 043613 (2006).
- [63] B. A. Malomed, F. Lederer, D. Mazilu, and D. Mihalache, On stability of vortices in three-dimensional selfattractive Bose-Einstein condensates, Phys. Let. A 361, 336 (2007).
- [64] G. Herring, L. D. Carr, R. Carretero-González, P. G. Kevrekidis and D. J. Frantzeskakis, Radially symmetric nonlinear states of harmonically trapped Bose-Einstein condensates, Phys. Rev. A, 77, 023625 (2008).
- [65] D. A. Zezyulin, Stability of two-dimensional radial excited states of a Bose-Einstein condensate in an anharmonic trap, Phys. Rev. A 79, 033622 (2009).
- [66] L. D. Carr and J. Brand, Multidimensional Solitons: Theory. In: Kevrekidis, P.G., Frantzeskakis, D.J., Carretero-González, R. (eds) Emergent Nonlinear Phenomena in Bose-Einstein Condensates. Atomic, Optical, and Plasma Physics, vol 45. Springer, Berlin, Heidelberg.
- [67] B. A. Malomed, Multidimensional solitons: Wellestablished results and novel findings, Eur. Phys. J. Spec. Top. 225, 2507 (2016).
- [68] V. A. Brazhnyi and V. V. Konotop, Evolution of a dark soliton in a parabolic potential: application to Bose-Einstein condensates, Phys. Rev. A 68, 043613 (2003).
- [69] D. E. Pelinovsky, D. J. Frantzeskakis, and P. G. Kevrekidis, Oscillations of dark solitons in trapped Bose-Einstein condensates, Phys. Rev. E 72, 016615 (2005).
- [70] D. E. Pelinovsky and P. G. Kevrekidis, Periodic oscillations of dark solitons in parabolic potentials, AMS Contemporary Mathematics (American Mathematical Society, Providence, 2008), Vol. 437, pp. 159-180.
- [71] Handbook of Mathematical Functions, edited by M. Abramovitz and I. A. Stegun (National Bureau of Standards, Washington, DC, 1972).
- [72] D. A. Zezyulin and V. V. Konotop, Nonlinear modes in the harmonic PT-symmetric potential, Phys. Rev. A 85, 043840 (2012).
- [73] D. A. Zezyulin and V. V. Konotop, Small-Amplitude Nonlinear Modes under the Combined Effect of the Parabolic Potential, Nonlocality and PT Symmetry,

- Symmetry 8, 72 (2016).
- [74] G. L. Alfimov, L. A. Gegel, M. E. Lebedev, B. A. Malomed, and D. A. Zezyulin, Localized modes in the Gross-Pitaevskii equation with a parabolic trapping potential and a nonlinear lattice pseudopotential, Commun. Nonlinear Sci. Numer. Simulat. 66, 194 (2019).
- [75] D. A. Zezyulin, G. L. Alfimov, V. V. Konotop, and V. M. Pérez-García, Control of nonlinear modes by scatteringlength management in Bose-Einstein condensates, Phys. Rev. A 76, 013621 (2007).
- [76] A. E. Kaplan, Bistable solitons, Phys. Rev. Lett. 55, 1291 (1985).
- [77] B. V. Gisin, R. Driben, and B. A. Malomed, Bistable guided solitons in the cubic-quintic medium, J. Opt. B: Quantum Semiclass. Opt. 6, S259-S264 (2004).
- [78] J. Yang, No stability switching at saddle-node bifurcations of solitary waves in generalized nonlinear Schrödinger equations, Phys. Rev. E 85, 037602 (2012).
- [79] N. G. Vakhitov and A. A. Kolokolov, Stationary solutions of the wave equation in a medium with nonlinearity sat-

- uration, Radiophys. Quantum Electron. **16**, 783 (1973) [Izvestiya Vysshikh Uchebnykh Zavedenii, Radiofizika, **16**, 1020 (1973)].
- [80] J. J. García-Ripoll, V. M. Pérez-García, and V. Vekslerchik, Construction of exact solutions by spatial translations in inhomogeneous nonlinear Schrödinger equations, Phys. Rev. E 64, 056602 (2001).
- [81] A. D. Martin, C. S. Adams, and S. A. Gardiner, Bright solitary-matter-wave collisions in a harmonic trap: Regimes of solitonlike behavior, Phys. Rev. A 77, 013620 (2008).
- [82] Hui Hu and Xia-Ji Liu, Consistent Theory of Self-Bound Quantum Droplets with Bosonic Pairing, Phys. Rev. Lett. 125, 195302 (2020).
- [83] Hui Hu, Jia Wang, and Xia-Ji Li, Hui Hu, Jia Wang, and Xia-Ji Li, Microscopic pairing theory of a binary Bose mixture with interspecies attractions: Bosonic BEC-BCS crossover and ultradilute low-dimensional quantum droplets, Phys. Rev. A 102, 043301 (2020).